1993

Longitudinal waves in homogeneous anisotropic cylindrical bars immersed in fluid

Vinay Dayal
Iowa State University, vdayal@iastate.edu

Longitudinal waves in homogeneous anisotropic cylindrical bars immersed in fluid

Abstract

The propagation of a longitudinal wave in an anisotropic cylindrical bar immersed in water is considered. Energy is leaked into the surrounding fluid in the form of traveling waves, and this leakage determines the amplitude of the signal in the rod. This aspect is important in nondestructive evaluation of composite rods. The governing equation of the longitudinal waves traveling in the rod is obtained and is solved numerically to obtain the dispersion curves and the attenuation, which is due to the energy leaked into the fluid. Results are presented for rods of five different materials.

Disciplines

Aerospace Engineering | Structures and Materials

Comments

This article is published as Dayal, Vinay. "Longitudinal waves in homogeneous anisotropic cylindrical bars immersed in fluid." *The Journal of the Acoustical Society of America* 93, no. 3 (1993): 1249-1255. doi: 10.1121/1.405409. Posted with permission.

Longitudinal waves in homogeneous anisotropic cylindrical bars immersed in fluid

Vinay Dayal
Aerospace Engineering and Engineering Mechanics, Iowa State University, Ames, Iowa 50011

(Received 6 January 1992; accepted for publication 23 November 1992)

The propagation of a longitudinal wave in an anisotropic cylindrical bar immersed in water is considered. Energy is leaked into the surrounding fluid in the form of traveling waves, and this leakage determines the amplitude of the signal in the rod. This aspect is important in nondestructive evaluation of composite rods. The governing equation of the longitudinal waves traveling in the rod is obtained and is solved numerically to obtain the dispersion curves and the attenuation, which is due to the energy leaked into the fluid. Results are presented for rods of five different materials.

PACS numbers: 43.20.Fn, 43.20.Hq, 43.40.Cw

INTRODUCTION

During the last few decades, composite materials have been used in a variety of applications, especially in the aerospace industry. The use of composites has been prompted by their properties, such as: excellent strength/weight and stiffness/weight ratios, good ability to tailor mechanical and thermal properties, high corrosion resistance, etc. The high cost of advanced composites tended to restrict their use to aerospace and sporting equipment products. Conventionally, composites have been used in plate or shell-like form. Recently, the construction industry has started taking interest in composites because of high tensile strength and excellent corrosion resistance properties. Steel rods in reinforced concrete pose a big corrosion problem that could be avoided by using composite rods. Cost considerations have restricted use to glass/epoxy systems, but as usage increases, cost is almost certain to come down. With the use of composite rods comes the problem of their testing and inspection. Ultrasonic waves are a possible means of nondestructive evaluation (NDE) of such rods.

The problem of stress waves propagating in a rod has been treated by Pochhammer,[1] who derived the dispersion equation for waves propagating in circular rods. Chree has written a series of papers on the longitudinal vibration of isotropic materials[2,3] and aeolotropic bars with one axis of material symmetry.[4] Various researchers have taken the dispersion equations derived by Pochhammer and developed the cases for short wavelength and long wavelength limits. Bancroft[5] has written the equations in terms of Poisson's ratio and the ratio of the diameter of the bar to the wavelength and obtained asymptotic values for the propagation velocities at very short wavelengths. Hudson[6] has redeveloped the theory of elastic vibrations in solid circular cylindrical rods of homogeneous isotropic materials. He has studied both longitudinal and flexural waves. Some experimental results are also reported. Davis[7] has performed extensive experiments on waves propagating in rods. Mindlin and McNiven[8] have derived approximate, one-dimensional equations coupling longitudinal, axial shear, and radial modes. Onoe *et al.*[9] have studied Pochhammer's equations and have developed spectra covering a large range of frequencies. Meitzler[10] has compared Pochhammer's equations for a rod and the Rayleigh–Lamb equations for a plate. He discusses the case where the group velocity and phase velocity are of opposite signs. Meeker and Meitzler[11] have written a review article on wave propagation in cylinders and plates.

Thus we see that Chree[4] was first to study vibrations in an anisotropic bar. He derived the equations for vibrations of a finite bar and dealt with the boundaries and reflections. In the work reported here, dispersion equations for an infinite homogeneous anisotropic bar immersed in fluid are derived. It is shown that Pochhammer's equations are a special case of the equations developed here. The equations are solved numerically and results are presented for rods immersed in water and made of isotropic, weakly anisotropic and anisotropic materials.

I. THEORY

The coordinate system used in this derivation is as shown in Fig. 1. Directions x (or 1) and y (or 2) are in the plane of the cross section and z (or 3) is along the axis of the cylinder. Displacements in the three directions are u, v, and w, respectively. The constitutive relation for an orthotropic material can be written as

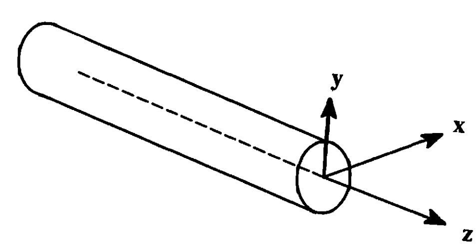

FIG. 1. The coordinate system used in the derivation of equations.

 0001-4966/93/031249-07$06.00

$$\begin{Bmatrix} \sigma_{xx} \\ \sigma_{yy} \\ \sigma_{zz} \\ \sigma_{yz} \\ \sigma_{xz} \\ \sigma_{xy} \end{Bmatrix} = \begin{bmatrix} c_{11} & c_{12} & c_{13} & 0 & 0 & 0 \\ c_{12} & c_{22} & c_{23} & 0 & 0 & 0 \\ c_{13} & c_{23} & c_{33} & 0 & 0 & 0 \\ 0 & 0 & 0 & c_{44} & 0 & 0 \\ 0 & 0 & 0 & 0 & c_{55} & 0 \\ 0 & 0 & 0 & 0 & 0 & c_{66} \end{bmatrix} \times \begin{Bmatrix} \dfrac{\partial u}{\partial x} \\ \dfrac{\partial v}{\partial y} \\ \dfrac{\partial w}{\partial z} \\ \dfrac{\partial v}{\partial z} + \dfrac{\partial w}{\partial y} \\ \dfrac{\partial u}{\partial z} + \dfrac{\partial w}{\partial x} \\ \dfrac{\partial u}{\partial y} + \dfrac{\partial v}{\partial x} \end{Bmatrix}. \tag{1}$$

The equation of motion, assuming no body forces acting, is given by

$$\sum_{j=1}^{3} \sigma_{ij,j} = \rho \ddot{U}_i. \tag{2}$$

Substituting Eq. (1) in Eq. (2), we get a set of three equations relating the three displacements

$$c_{11} \frac{\partial^2 u}{dx^2} + c_{12} \frac{\partial^2 v}{\partial x\, \partial y} + c_{13} \frac{\partial^2 w}{\partial x\, \partial z} + c_{66}\left(\frac{\partial^2 w}{dy^2} + \frac{\partial^2 v}{\partial x\, \partial y}\right) + c_{55}\left(\frac{\partial^2 u}{\partial z^2} + \frac{\partial^2 w}{\partial x\, \partial z}\right) = \rho \ddot{u}, \tag{3a}$$

$$c_{66}\left(\frac{\partial^2 u}{\partial x\, \partial y} + \frac{\partial^2 v}{dx^2}\right) + c_{12} \frac{\partial^2 u}{\partial x\, \partial y} + c_{22} \frac{\partial^2 v}{dy^2} + c_{23} \frac{\partial^2 w}{\partial x\, \partial y} + c_{44}\left(\frac{\partial^2 v}{\partial z^2} + \frac{\partial^2 w}{\partial y\, \partial z}\right) = \rho \ddot{v}, \tag{3b}$$

and

$$c_{55}\left(\frac{\partial^2 u}{\partial x\, \partial z} + \frac{\partial^2 w}{dx^2}\right) + c_{44}\left(\frac{\partial^2 v}{\partial y\, \partial z} + \frac{\partial^2 w}{dy^2}\right) + c_{13} \frac{\partial^2 u}{\partial x\, \partial z} + c_{23} \frac{\partial^2 v}{\partial y\, \partial z} + c_{33} \frac{\partial^2 w}{dz^2} = \rho \ddot{w}. \tag{3c}$$

From symmetry of the circular rod, we have that the displacements u in the x direction, v in the y direction, and U_r in the radial direction are related by

$$\frac{u}{x} = \frac{v}{y} = \frac{U_r}{r} \quad \text{where} \quad r^2 = x^2 + y^2.$$

We analyze here materials possessing transversely isotropic symmetry and thus $c_{66} = (c_{11} - c_{12})/2$. It is assumed that displacement in the hoop direction, U_θ is zero. Equations (3a) and (3b) reduce to

$$c_{11}\left(\frac{\partial^2 U_r}{\partial r^2} + \frac{1}{r} \frac{\partial U_r}{\partial r} - \frac{U_r}{r^2}\right) + (c_{13} + c_{55}) \frac{\partial^2 w}{\partial r\, \partial z} + c_{55} \frac{\partial^2 U_r}{\partial z^2} - \rho \ddot{U}_r = 0. \tag{4}$$

Similarly, Eq. (3c) can be written as

$$(c_{13} + c_{44})\left[\frac{\partial}{\partial z}\left(\frac{U_r}{r} + \frac{\partial U_r}{\partial r}\right)\right] + c_{44}\left(\frac{\partial^2 w}{\partial r^2} + \frac{1}{r} \frac{\partial w}{\partial r}\right) + c_{33} \frac{\partial^2 w}{\partial z^2} - \rho \ddot{w} = 0. \tag{5}$$

Equations (4) and (5) couple the radial and axial displacements. These equations can easily be decoupled by the use of displacement potentials. Since we are deriving the equations for longitudinal displacements, the rod being circular, and the material transversely isotropic, the angular dependence in displacements can be set to zero. Thus

$$U_r = \frac{\partial \phi}{\partial r} - \frac{\partial \psi_\theta}{\partial z} \quad \text{and} \quad w = \frac{\partial \phi}{\partial z} + \frac{1}{r} \frac{\partial (r\psi_\theta)}{\partial r}. \tag{6}$$

Substituting Eq. (6) in Eq. (4) and collecting like terms, we obtain

$$\frac{\partial}{\partial r}\left[c_{11}\left(\frac{\partial^2 \phi}{\partial r^2} + \frac{1}{r} \frac{\partial \phi}{\partial r}\right) + (c_{13} + 2c_{55}) \frac{\partial^2 \phi}{\partial z^2} - \rho \ddot{\phi}\right] + \frac{\partial}{\partial z}\left[(c_{13} + c_{55} - c_{11})\left(\frac{\partial^2 \psi_\theta}{\partial r^2} + \frac{1}{r} \frac{\partial \psi_\theta}{\partial r} - \frac{\psi_\theta}{r^2}\right) - c_{55} \frac{\partial^2 \psi_\theta}{\partial z^2} + \rho \ddot{\psi}_\theta\right] = 0. \tag{7}$$

Equation (7) will be fully satisfied if the terms under the braces are both equal to zero, see Davis.[12] Then,

$$c_{11}\left(\frac{\partial^2 \phi}{\partial r^2} + \frac{1}{r} \frac{\partial \phi}{\partial r}\right) + (c_{13} + 2c_{55}) \frac{\partial^2 \phi}{\partial z^2} - \rho \ddot{\phi} = 0 \tag{8}$$

and

$$(c_{13} + c_{55} - c_{11})\left(\frac{\partial^2 \psi_\theta}{\partial r^2} + \frac{1}{r} \frac{\partial \psi_\theta}{\partial r} - \frac{\psi_\theta}{r^2}\right) - c_{55} \frac{\partial^2 \psi_\theta}{\partial z^2} + \rho \ddot{\psi}_\theta = 0. \tag{9}$$

Longitudinal waves traveling in the rod can be visualized as standing waves in the radial direction and propagating waves in the axial direction. Hence, the displacement potentials can be assumed to be of the following form:

$$\phi = \Phi(r) \exp[i(kz - \omega t)], \tag{10}$$

where k is the wave number, ω is the circular frequency, and t is the time.

Substituting Eq. (10) in (8) and dividing by c_{11}, the following is obtained:

$$\Phi''(r) + \frac{1}{r} \Phi'(r) + \frac{\rho\omega^2 - k^2(c_{13} + 2c_{55})}{c_{11}} \Phi(r) = 0. \tag{11}$$

This equation is Bessel's equation of the first kind with $n = 0$, and, in general, can be written as

$$\Phi''(r) + \frac{1}{r} \Phi'(r) + \left(\gamma^2 - \frac{n^2}{r^2}\right)\Phi(r) = 0, \tag{12}$$

where

$$\gamma^2 = \frac{\rho\omega^2 - k^2(c_{13} + 2c_{55})}{c_{11}} \quad \text{and} \quad n = 0.$$

The solution of Eq. (12), which is nonsingular at the origin, is given by

$$\Phi(r) = AJ_0(\gamma r). \tag{13}$$

The potential ψ_θ is also assumed to be of the type

$$\psi_\theta = \Psi_\theta(r)\exp[i(kz-\omega t)]. \tag{14}$$

Substitute Eq. (14) in Eq. (9) and divide by $(c_{13}+c_{55}-c_{11})$ to obtain the different equation

$$\Psi_\theta'' + \frac{1}{r}\Psi_\theta' + \left(\frac{c_{55}k^2-\rho\omega^2}{c_{13}+c_{55}-c_{11}} - \frac{n^2+1^2}{r^2}\right)\Psi_\theta = 0. \tag{15}$$

This is also a Bessel's equation of the first kind,

$$\Psi_\theta'' + \frac{1}{r}\Psi_\theta' + \left(\eta^2 - \frac{n^2+1^2}{r^2}\right)\Psi_\theta = 0, \tag{16}$$

where

$$\eta^2 = \frac{c_{55}k^2-\rho\omega^2}{c_{13}+c_{55}-c_{11}} \quad \text{and} \quad n=0.$$

The solution of Eq. (16) is the Bessel's function $J_l(\eta r)$.

Hence, a longitudinal wave propagating in the composite rod can be expressed by a set of potentials

$$\Phi = AJ_0(\gamma r)\exp[i(kz-\omega t)]$$

and (17)

$$\psi_\theta = BJ_1(\eta r)\exp[i(kz-\omega t)],$$

where A and B are arbitrary constants.

The potentials ϕ and ψ_θ can now be used to obtain the displacements from Eq. (6) as

$$U_r = [-A\gamma J_1(\gamma r) - BJ_1(\eta r)ik]\exp[i(kz-\omega t)]$$

and (18)

$$w = [AikJ_0(\gamma r) + B\eta J_0(\eta r)]\exp[i(kz-\omega t)].$$

The constants A and B can be obtained by application of the boundary conditions

$$\sigma_{rr} = -p \quad \text{at} \quad r=a, \tag{19}$$

$$\sigma_{rz} = 0 \quad \text{at} \quad r=a. \tag{20}$$

Physically, this means that the radial stress σ_{rr} equals the pressure p in the fluid, and since the fluid cannot sustain shear σ_{rz} is zero at the boundary. In addition, continuity of displacement means that the particle displacements of the rod and fluid will be the same at the interface, or,

$$U_r = W_L \quad \text{at} \quad r=a. \tag{21}$$

The boundary conditions, Eqs. (19) and (20), can be written in terms of displacements as

$$c_{11}\frac{\partial U_r}{\partial r} + c_{12}\frac{U_r}{r} + c_{13}\frac{\partial w}{\partial z} = -p \quad \text{at} \quad r=a \tag{22}$$

and

$$\frac{\partial U_r}{\partial z} + \frac{\partial w}{\partial r} = 0 \quad \text{at} \quad r=a. \tag{23}$$

Substituting the displacements U_r and w from Eq. (18) into Eq. (22) and multiplying both sides by $a/(c_{11}-c_{12})$, we obtain

$$A\left(\gamma J_1(\gamma a) - \frac{c_{11}\gamma^2+c_{13}k^2}{c_{11}-c_{12}}aJ_0(\gamma a)\right) + B\left(ikJ_1(\eta a) - \frac{c_{11}-c_{13}}{c_{11}-c_{12}}ik\eta aJ_0(\eta a)\right) = -\frac{pa}{c_{11}-c_{12}}. \tag{24}$$

Similarly, Eq. (23) gives

$$-A\,2\gamma J_1(\gamma a)ik + B(k^2-\eta^2)J_1(\eta a) = 0. \tag{25}$$

Pressure waves in the fluid can be written in the form of a potential ϕ_L which will satisfy

$$\frac{\partial^2\phi_L}{\phi r^2} + \frac{1}{r}\frac{\partial\phi_L}{\partial r} + \frac{\partial^2\phi_L}{\partial z^2} + k_L^2\phi_L = 0, \tag{26}$$

where $k_L = \omega/c_L$ is the wave number in water. The form of ϕ_L in the fluid, which satisfies Eq. (26), will be of the type $\phi_L = \phi_0\exp[i(k_{rL}r + kz - \omega t)]$. It can be visualized that the waves will be traveling radially with a velocity of C_{rL} ($k_{rL} = \omega/C_{rL}$) and in the z direction the velocity of the wave will be the same in the liquid and rod. Then, by substitution of ϕ_L in Eq. (26), the radial wave number in the fluid can be obtained from

$$rk_{rL}^2 - ik_{rL} + r(k^2-k_L^2) = 0. \tag{27}$$

The displacement in the fluid W_L can be determined from

$$W_L = \frac{\partial\phi_L}{\partial r}.$$

Applying the displacement boundary condition Eq. (21) to the above equation, we get

$$[-A\gamma J_1(\gamma a) - BJ_1(\eta a)ik] = i\phi_0 k_{rL}\exp(ik_{rL}a). \tag{28}$$

The pressure in the fluid can now be written as

$$p = \lambda_L\nabla^2\phi_L = -\lambda_L k_L^2\phi_L, \tag{29}$$

where $\lambda_L = \rho_L c_L^2$, ρ_L is the density of the fluid, c_L is the wave speed in the fluid and ϕ_L is the fluid potential, then,

$$p(r=a) = -\rho_L\omega^2\phi_0\exp[i(k_La + kz - \omega t)]. \tag{30}$$

Substituting Eq. (30) in Eq. (24), we get

$$A\left(\gamma J_1(\gamma a) - \frac{c_{11}\gamma^2+c_{13}k^2}{c_{11}-c_{12}}aJ_0(\gamma a) + \frac{a\rho_L\omega^2}{c_{11}-c_{12}}\frac{\gamma J_1(\gamma a)}{ik_{rL}}\right) + B\left(J_1(\eta a) - \frac{c_{11}-c_{13}}{c_{11}-c_{12}}\eta aJ_0(\eta a) + \frac{a\rho_L\omega^2}{c_{11}-c_{12}}\frac{J_1(\eta a)}{ik_{rL}}\right)ik = 0. \tag{31}$$

Now, Eqs. (25) and (31) form a set of equations, and for a nontrivial solution, the following determinant should vanish:

$$\begin{bmatrix} \gamma J_1(\gamma a) - \dfrac{c_{11}\gamma^2 + c_{13}k^2}{c_{11} - c_{12}} aJ_0(\gamma a) + \dfrac{a\rho_L\omega^2}{c_{11} - c_{12}} \dfrac{\gamma J_1(\gamma a)}{ik_{rL}} & ik\, J_1(\eta a) - \dfrac{c_{11} - c_{13}}{c_{11} - c_{12}} \eta a J_0(\eta a) + \dfrac{a\rho_L\omega^2}{c_{11} - c_{12}} \dfrac{J_1(\eta a)}{ik_{rL}} \\ -2\gamma J_1(\gamma_a) ik & (k^2 - \eta^2) J_1(\eta a) \end{bmatrix} = 0. \quad (32)$$

Let $xJ_0(x)/J_1(x) = \chi(x)$, $\gamma^2 = p^2k^2$, and $\eta^2 = q^2k^2$, and substituting these into Eq. (32), simplification yields

$$p^2(q^2+1) + (1-q^2)\frac{c_{11}p^2 + c_{13}}{c_{11} - c_{12}}\chi(pka) - \frac{c_{11} - c_{13}}{c_{11} - c_{12}} 2p^2\chi(qka) = \frac{ia\rho_L\omega^2 p^2(1+q^2)}{(c_{11} - c_{12})k_{rL}}, \quad (33)$$

which is the dispersion equation for an anisotropic rod immersed in a fluid of density ρ_L. Here,

$$p^2 = (\rho c^2 - c_{13} - 2c_{55})/c_{11},$$
$$q^2 = (c_{55} - \rho c^2)/(c_{13} + c_{55} - c_{11}).$$

Equation (33) can be reduced for an isotropic material by substituting $c_{11} = \lambda + 2\mu$, $c_{12} = \lambda$, $c_{13} = \lambda$, and $c_{55} = \mu$, as

$$\left(\frac{c^2}{c_1^2} - 1\right)\frac{c^2}{c_t^2} + \left(2 - \frac{c^2}{c_t^2}\right)\frac{(\lambda + 2\mu)[(c^2/c_1^2) - 1] + \lambda}{2\mu}\chi(pka) - 2\left(\frac{c^2}{c_1^2} + 1\right)\chi(qka) = \frac{ia\rho_L\omega^2[(c^2/c_1^2) - 1](c^2/c_t^2)}{2\mu k_{rL}}. \quad (34)$$

It is not difficult to show that the function $\chi(x) \to x$ for large values of x, or, in Eq. (34), $\chi(pka) \to pka$, which in turn means that ka is large or we approach the Rayleigh wave-speed limit. Then, for

$$s = \frac{c_t^2}{c^2}, \quad t = \frac{c_t^2}{c_1^2}, \quad r = \frac{c_t^2}{c_L^2}, \quad k_{rL}^2 = k_L^2 - k^2,$$

Eq. (34) can be reduced to

$$(2s-1)^2 - 4s\sqrt{s-1}\sqrt{s-t} = -i\frac{\rho_L}{\rho}\sqrt{\frac{s-t}{r-s}}, \quad (35)$$

which is the same as obtained by Viktorov *et al.*[13]

There are two limiting cases which are of interest.

A. Case I

Here, the wavelength is large in comparison with the radius and $ka \to 0$. It can be shown that

$$\lim_{k \to 0} \chi(x) = 2. \quad (36)$$

Equation (36) is substituted in Eq. (33) to obtain the expression for the bar velocity in the composite rod

$$2\left(\frac{c_{13} + c_{11}p^2}{c_{11} - c_{12}}\right)(q^2 - 1) = p^2\left(q^2 + 1 - \frac{4(c_{11} - c_{13})}{c_{11} - c_{12}}\right). \quad (37)$$

Some manipulation of this equation provides the bar velocity in the following form:

$$c_b^2 = \frac{c_{11}}{\rho}\left(M - \frac{(2+L)(D-C) + \sqrt{(2+L)^2(D-C)^2 - 4C\{(C-D)L - 2D + C\}}}{2CL}\right), \quad (38)$$

where c_b is the bar velocity, and

$$C = \frac{c_{11} + c_{12}}{c_{11} - c_{12}}, \quad D = \frac{2c_{13}}{c_{11} - c_{12}},$$

$$L = \frac{c_{11}}{c_{13} + c_{55} - c_{11}}, \quad M = \frac{c_{55}}{c_{11}}.$$

B. Case II

Here, we analyze the case where $ka \to \infty$. We approach the Rayleigh wave speed from below, i.e., the wavelength is very small in comparison with the bar radius. This means that p and q will be complex. From Ref. 14

$$Jn(ix) = In(x), \quad n = 0,4,8,$$
$$= iIn(x), \quad n = 1,5,9. \quad (39)$$

Then, in the limit,

$$\lim_{x \to \infty} \chi(ix) = x. \quad (40)$$

Substitute Eq. (40) in (33) and let $ka \to \infty$, the equation is reduced to

$$(1-q^2)(c_{11}p^2 + c_{13}) - 2(c_{11} - c_{13})pq = i\rho_L cp(1+q^2)/C_{rL}. \quad (41)$$

For the isotropic case Eq. (41) reduces to Eq. (35). Solution of Eq. (41) gives the complex Raleigh wave in the fluid. The complex part is due to the leaking of energy into the fluid.

TABLE I. Properties of various materials.

Material	c_{11}/ρ	c_{33}/ρ	c_{55}/ρ	c_{13}/ρ	c_{12}/ρ	ρ
A1, isotropic	3.97	3.97	0.73	2.51	2.51	2.70
Mg, polycrystalline	3.42	3.55	0.95	1.47	1.23	1.74
Cu, polycrystalline	2.24	2.22	0.53	1.20	1.19	8.93
Th300/914 ep	1.00	9.72	0.47	0.23	0.27	1.60
Gl/Ep	1.04	3.00	0.47	0.33	0.29	1.90

II. RESULTS AND DISCUSSION

It is obvious that Eq. (33) for the dispersion curve, Eq. (38) for the bar velocity, and Eq. (41) for the Rayleigh wave speed are complicated and complex and simplification, if any, will not lead to any greater insight into the behavior of the equations. Hence, a computational approach has been taken to solve these equations.

The equations were applied to five different types of materials, both metallic and composite. Various properties of these materials are listed in Table I.

To check the validity of the equations derived here, we have used the data for an aluminum rod. The dispersion curves for the aluminum rod are plotted in Fig. 2(a), as nondimensional phase velocity, c/c_b, against frequency multiplied by rod radius a. Solid lines show the dispersion curves in air, and the dashed line in water. It can be observed that except for the first mode, all higher modes have a cutoff frequency, i.e., they do not exist below the cutoff frequency. The dispersion curves for water are not shown fully because over larger parts they fall on the curves for air. Only areas

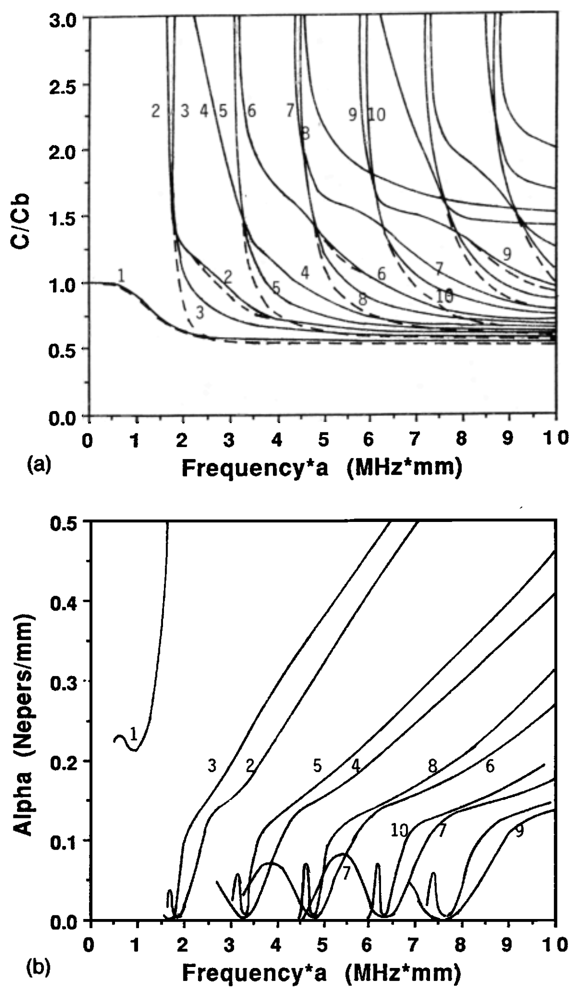

FIG. 2. (a) The dispersion curves and (b) the leaky attenuation curves for an aluminum rod immersed in water.

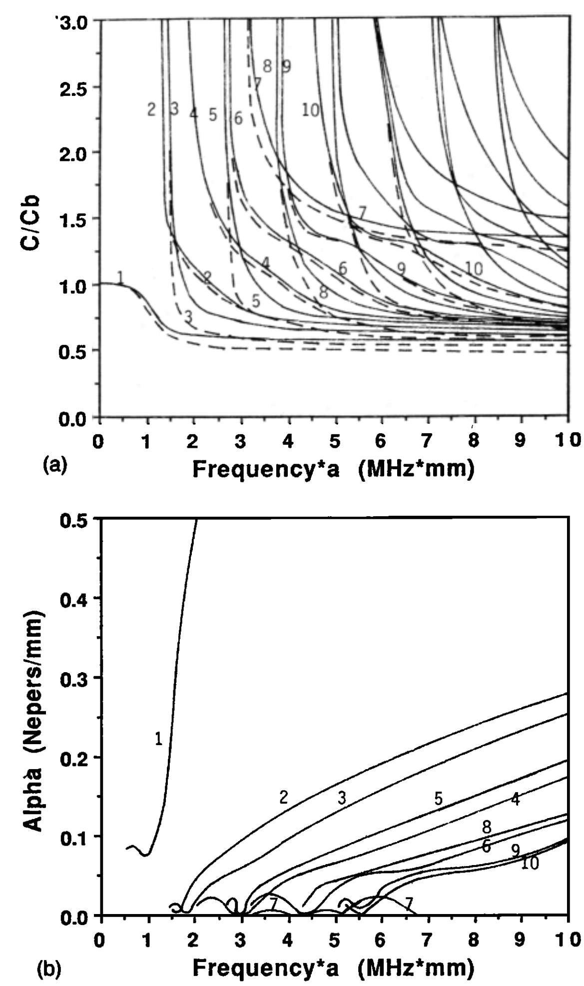

FIG. 3. (a) The dispersion curves and (b) the leaky attenuation curves for a Polycrystal copper rod immersed in water. The material is weakly anisotropic.

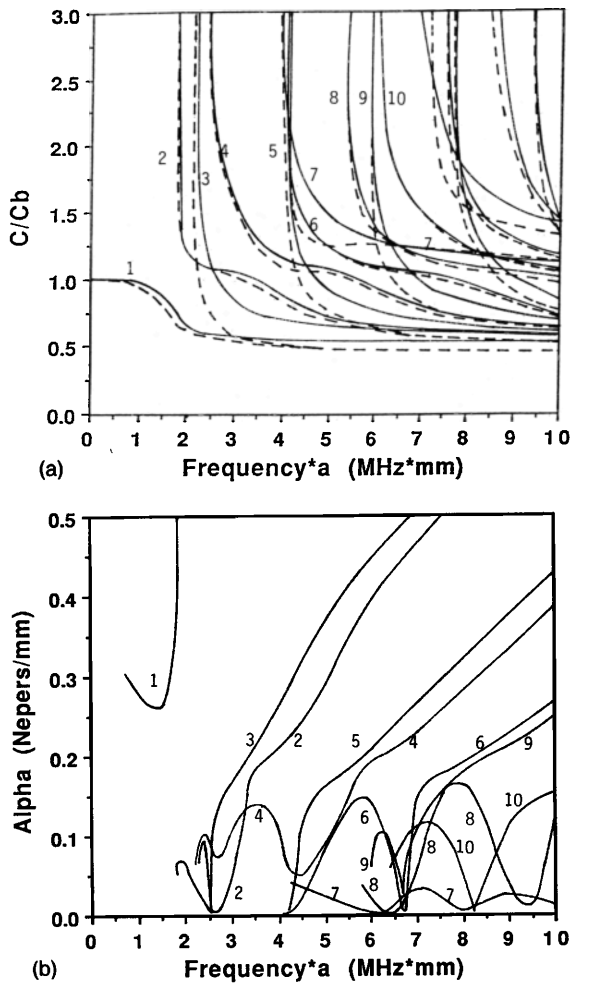

FIG. 4. (a) The dispersion curves and (b) the leaky attenuation curves for a magnesium rod immersed in water.

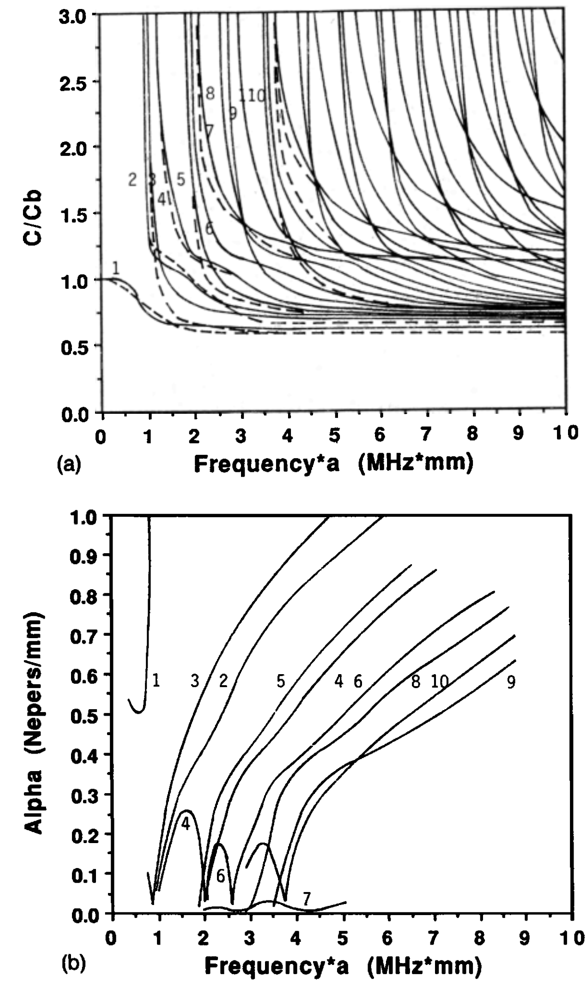

FIG. 5. (a) The dispersion curves and (b) the leaky attenuation curves for a Th300/914 epoxy rod immersed in water.

where they are different are shown. It is observed that near the cutoff frequency, the effect of water loading is minimal. As the frequency increases, the effect of water loading becomes pronounced on some modes and does not affect others. The waves tend to approach the Rayleigh wave limit more rapidly than when the rod is in air. The bar velocity, c_b obtained from Eq. (38) and the Rayleigh wave speed c_r obtained from Eq. (41), exactly match the two limiting cases, validating the equations here in the limits. The dispersion curve for an aluminum rod in air matches exactly with the data obtained by Davis.[7] Figure 2(b) shows the attenuation coefficient α plotted against frequency *a. The values show that attenuation is small near the cutoff frequency but then increases rapidly. As the limit for the Rayleigh wave speed is approached, the attenuation becomes very high. This is obvious as the Rayleigh waves are confined to the outer surface of the rod. It may also be noted that the attenuation presented here is assumed to consist mainly of the leak of energy from the rod into the fluid. When the attenuation of an immersed rod is compared to the attenuation of a plate of the same material in water, Dayal *et al.*,[15] it is observed that the attenuation or leakage from the rod is, in general, much higher than that from the plate. The reason is quite obvious, the plate has only the top and bottom surfaces to radiate energy while the rod has the entire circumferential surface to do so.

The dispersion and attenuation curves for a polycrystalline copper rod are shown in Fig. 3. As can be seen from the properties, Table I, the material is weakly anisotropic and has a very high density in comparison with aluminum. It is observed that the effect of fluid loading is larger on the dispersion curves but the attenuation curves show lower values. The leak of energy into the fluid is lower as the density of the rod is higher. Figure 4 shows the dispersion curves for polycrystalline magnesium rods. It is observed from the data that this material is also weakly anisotropic and though the c_{11}/ρ and c_{33}/ρ are comparable to the values for aluminum, the density is much lower. Dispersion curves show some effect of fluid loading, a little more than the aluminum rod, but less than the copper. On the other hand, the attenuation is significantly higher. The reason for higher attenuation is the very low density which is now comparable to the surrounding medium.

The dispersion curves for highly anisotropic composites are presented next. Figure 5 shows the dispersion and attenuation curves for glass/epoxy composite rods. The material is highly anisotropic. It is observed that the effect of fluid loading is significant on various modes and the attenuation is

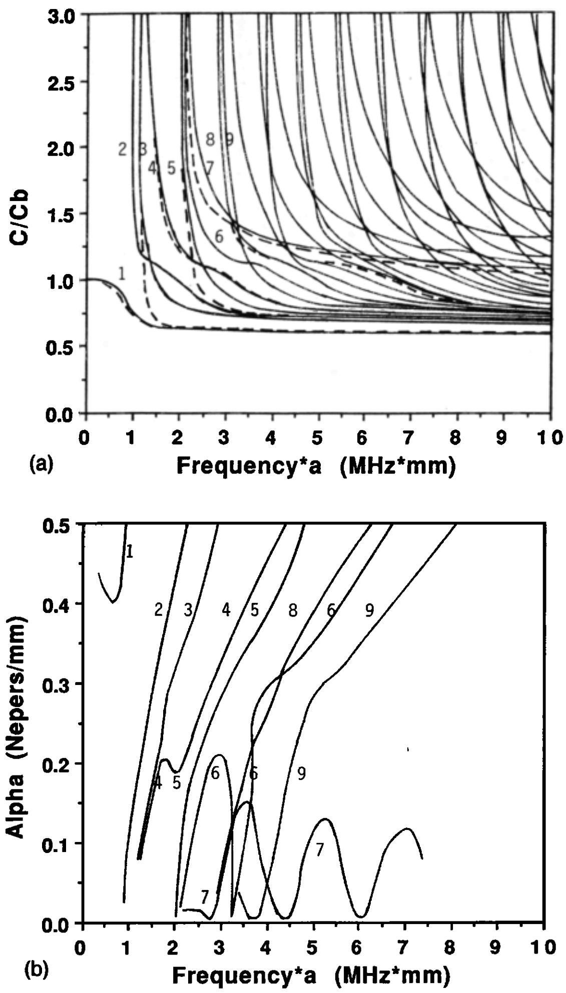

FIG. 6. (a) The dispersion curves and (b) the leaky attenuation curves for a glass epoxy rod immersed in water.

high. Finally, Fig. 6 presents the dispersion and attenuation curves for Thornel T300/919 epoxy. This material is highly anisotropic, ($c_{33}/c_{11} = 9.75$, as compared to 2.87 for glass/epoxy), while the densities are comparable. The effect of fluid loading on the dispersion is more than that for glass epoxy and the attenuations are comparable.

Comparison of the attenuation of the five materials presented here shows that the attenuation is directly correlated to the density of the materials. Copper with the highest density has the minimum attenuation, aluminum has the next higher attenuation, and the other three with comparable densities have highest attenuation. The magnesium rod has slightly lower density than glass/epoxy, but has higher stiffness and hence a small reduction in attenuation.

III. CONCLUSIONS

The dispersion equations for a longitudinal wave in a homogeneous, anisotropic cylindrical bar immersed in a fluid are derived. These have been solved by numerical methods. It is observed that near the cutoff frequencies fluid loading has no significant effect but as the wave mode changes from the bar mode to the Rayleigh mode, the effect of fluid loading becomes significant, and also, the attenuation caused by the leakage of energy into the surrounding medium increases dramatically. The attenuation is lower for materials with higher density.

[1] L. Pochhammer, "Ueber die Fortpflanzungsgeschwindigkeinten Schwingungen in einem unbegrenzten isotropen Kreiscylinder," Z. Math. **81**, 326–336 (1876).

[2] C. Chree, "Longitudinal Vibrations of a Circular Bar," Q. J. Math. **21**, 287–298 (1886).

[3] C. Chree, "On Longitudinal Vibrations," Q. J. Math. **23**, 317–342 (1889).

[4] C. Chree, "On the Longitudinal Vibrations of Aelotropic Bars with one Axis of Material Symmetry," Q. J. Math. **24**, 340–358 (1890).

[5] D. Bancroft, "The Velocity of Longitudinal Waves in Cylindrical Bars," Phys. Rev. **59**, 588–593 (April 1941).

[6] G. E. Hudson, "Dispersion of Elastic Waves in Solid Circular Cylinders," Phys. Rev. **63**, 46–51 (Jan. 1943).

[7] R. M. Davies, "A Critical Study of the Hopkinson Pressure Bar," Philos. Trans. R. Soc. London, Ser. A **240**(821), 375–457 (Jan. 1948).

[8] R. D. Mindlin and H. D. McNiven, "Axially Symmetric Waves in Elastic Rods," J. Appl. Mech. Ser. E **27**(1), 145–196 (March 1960).

[9] M. Onoe, H. D. McNiven, and R. D. Mindlin, "Dispersion of Axially Symmetric Waves in Elastic Rods," J. Appl. Mech. Ser. E **29**(4), 729–734 (Dec. 1962).

[10] A. H. Meitzler, "Backward-Wave Transmission of Stress Pulses in Elastic Cylinders and Plates," J. Acoust. Soc. Am. **38**, 835–842 (1935).

[11] T. R. Meeker and A. H. Meitzler, "Guided Wave Propagation in Elongated Cylinders and Plates," in *Physical Acoustics*, edited by W. P. Mason (Academic, New York, 1964), Vol. 1.

[12] J. L. Davis, *Wave Propagation in Solids and Fluids* (Springer-Verlag, New York, 1988), pp. 297–299.

[13] I. A. Viktorov, E. K. Grishchenko, and T. M. Kaekina, Sov. Phys. Acoust. **9**(2) (1963).

[14] J. Spanier and K. B. Oldham, *An Atlas of Functions* (Hemisphere, New York, 1987).

[15] V. Dayal and V. K. Kinra, "Leaky Lamb waves in an isotropic plate. I: An exact solution and experiments," J. Acoust. Soc. Am. **85**, 2268–2276 (1989).